The influence of long-range links on spiral waves and their application for control*

Qian Yu(钱 郁)†

Nonlinear Research Institute, Baoji University of Arts and Sciences, Baoji 721007, *China*

(Received 2 February 2012; revised manuscript received 29 February 2012)

The influence of long-range links on spiral waves in an excitable medium has been investigated. Spatiotemporal dynamics in an excitable small-world network transform remarkably when we increase the long-range connection probability P. Spiral waves with few perturbations, broken spiral waves, pseudo spiral turbulence, synchronous oscillations, and homogeneous rest state are discovered under different network structures. Tip number is selected to detect non-equilibrium phase transition between different spatiotemporal patterns. The Kuramoto order parameter is used to identify these patterns and explain the emergence of the rest state. Finally, we use long-range links to successfully control spiral waves and spiral turbulence.

Keywords: spiral waves, long-range link, spiral and turbulence control

PACS: 82.40.Ck, 05.65.+b, 87.18.Bb, 89.75.Hc **DOI:** 10.1088/1674-1056/21/8/088201

1. Introduction

Spatiotemporal pattern formation in regular excitable media has attracted great attention during the last thirty years. The spiral wave is one of the most important and typical spatiotemporal patterns in excitable media due to its popular existence and potential application in various real systems,[1,2] such as the Belousov–Zhabotinsky (BZ) reactions,[3−5] the catalytic surface processes, and the cardiac tissue.[6−8] A spiral wave can self-sustain in an autonomous regular system with the spiral tip serving as the oscillation source. The dynamics of a spiral wave are not always stable and can change dramatically with the variation of the environment. A spiral wave is beautiful, but sometimes it is undesirable because of its harmfulness in the cardiac system. Lots of theoretic and experimental studies show that a spiral wave in cardiac muscle can be a cause of tachycardia. Repetitious breakup of a spiral wave due to Doppler instability can lead to spatiotemporal turbulence, which is believed to be a mechanism of ventricular fibrillation. Ventricular fibrillation and sudden cardiac death are the leading cause of cardiovascular mortality in industrialized countries.[9−11] Therefore, lots of methods have been proposed to control the spiral wave and spiral turbulence in excitable media.[12−21]

For many real systems, such as biological tissues,[22,23] neural networks,[24−27] and brain systems,[28−30] the topological structures are not regular but "small-world".[31] Long-range links cannot be neglected in these systems and do play a very important role in determining the dynamic behaviors of the given systems.[32−37] Spiral waves which are widespread in regular excitable media can also be observed in the mammalian neocortex which has a small-world network structure[29] and spiral waves in this kind of system will certainly be influenced by long-range links. Therefore, spiral dynamics in excitable small-world networks has become a hot issue in physical and biological fields and some research has been done in recent years. He *et al.* found that spiral patterns can be maintained in an inhomogeneous excitable medium with suitable long-range links.[32] The problem of non-equilibrium phase transition of spiral waves induced by system parameters has been studied in regular excitable media,[38] however, the transitions in an excitable small-world network due to the long-range connection probability are still unclear. This is what we will discuss in the present paper.

In this article we focus on the non-equilibrium phase transition of spiral waves induced by small-world connections and try to control the spiral wave and spiral turbulence by long-range links. By increasing the long-range connection probability P, spatiotemporal dynamics in an excitable small-world net-

*Project supported by the National Natural Science Foundation of China (Grant No. 11105003) and the Science Foundation of the Education Bureau of Shaanxi Province of China (Grant No. 11JK0544).

†Corresponding author. E-mail: qianyu0272@163.com

© 2012 Chinese Physical Society and IOP Publishing Ltd

work transform remarkably. Five distinct spatiotemporal patterns, i.e., spiral waves with few perturbations, broken spiral waves, pseudo spiral turbulence, synchronous oscillations, and homogeneous rest state, have been found under different network structures. Spiral tip number is selected to detect non-equilibrium phase transition between different spatiotemporal patterns. The Kuramoto order parameter is used to identify these patterns and explain the emergence of the rest state. The critical points can be clearly revealed by these two parameters. Finally, we can use long-range links to control spiral waves and spiral turbulence effectively. The system parameter-dependent control critical probability is also given.

2. Model and results

We take the two-dimensional Bär–Eiswirth[39] model as our example throughout this paper, and the activator u and inhibitor v satisfy the following equation

$$\dot{u}_{i,j} = -\frac{1}{\varepsilon}u_{i,j}(u_{i,j}-1)\left(u_{i,j}-\frac{v_{i,j}+b}{a}\right)+D_{i,j}, \quad (1)$$

$$\dot{v}_{i,j} = f(u_{i,j})-v_{i,j}, \quad (2)$$

$$D_{i,j} = D_u(u_{i-1,j}+u_{i+1,j}+u_{i,j-1} + u_{i,j+1}-4u_{i,j}), \quad (3)$$

where $i,j=1,\ldots,100$. The function $f(u)$ takes the form $f(u)=0$ for $u<1/3$; $f(u)=1-6.75u(u-1)^2$ for $1/3\le u\le 1$; and $f(u)=1$ for $u>1$. The small relaxation parameter ε represents the time ratio between activator u and inhibitor v, and a and b are two other parameters of the system. D_u is the diffusion coefficient of activator u. The system parameters are kept as $a=0.84$, $b=0.07$, $\varepsilon=0.04$, and $D_u=1.0$ unless noted elsewhere.

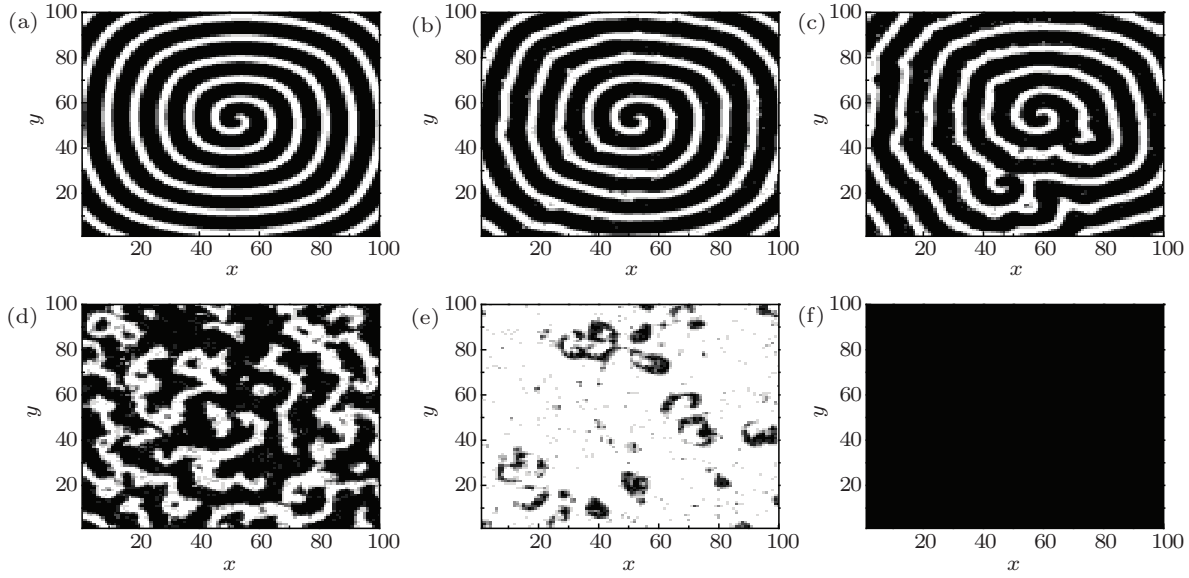


Fig. 1. (a) A perfect spiral wave is used as initial condition. Panels 1(b), 1(c), 1(d), 1(e), and 1(f) are five asymptotic spatiotemporal patterns realized at different long-range link probabilities P: (b) spiral wave with few perturbations at $P=0.05$, (c) broken spiral wave at $P=0.07$, (d) pseudo-spiral turbulence at $P=0.40$, (e) synchronous oscillation at $P=0.70$, and (f) homogeneous rest state at $P=0.90$.

To study the influence of long-range links on a spiral wave, we use a perfect spiral shown in Fig. 1(a) as our initial condition. The long-range links are introduced such that each excitable node receives a unidirectional connection from a randomly chosen node in the two-dimensional (2D) space with connection probability P. These long-range links are chosen initially and kept during the evolvement of the system. Therefore, an additional coupling term $D'_{i,j}$ is added to Eq. (1) to represent the long-range link as

$$\dot{u}_{i,j} = -\frac{1}{\epsilon}u_{i,j}(u_{i,j}-1)\left(u_{i,j}-\frac{v_{i,j}+b}{a}\right) + D_{i,j}+D'_{i,j}, \quad (4)$$

$$D'_{i,j} = D_u(u_{i',j'}-u_{i,j}). \quad (5)$$

Here node (i',j') is randomly chosen in the two-dimensional (2D) space. These equations are integrated by the second-order Runge–Kutta scheme with the time step $\Delta t=0.031$ and no-flux boundary condition is used.

By increasing the long-range connection probability, the spatiotemporal dynamics of the spiral wave transform remarkably. For further investigation, we randomly take fifty samples with different small-world network structures under each connection probability P. The spiral dynamics can be reflected by the number of spiral tips. We count the number of spiral tips in the spatiotemporal pattern at every time step and calculate the time average in each sample which is represented by $\langle N_{\rm tip}\rangle$. In this paper we use symbol $\langle\ \rangle$ representing time average and use $\langle N_{\rm tip}\rangle$ as an order parameter to detect the non-equilibrium phase transition of spiral waves induced by long-range links. When the spiral pattern is perfect, there must be only one tip in the medium and $\langle N_{\rm tip}\rangle$ equals one. While when spiral waves break up, the number of spiral tips will increase and $\langle N_{\rm tip}\rangle$ must be great than one. The distributions of $\langle N_{\rm tip}\rangle$ versus the long-range connection probability P are plotted by black dots in Fig. 2(a). For small connection probability (i.e., $P \leq 0.06$) $\langle N_{\rm tip}\rangle$s in the fifty samples are all equal to one, that is to say, spiral waves under these network structures are stable. A snapshot of spatiotemporal pattern at $P = 0.05$ is shown in Fig. 1(b). Long-range links under small connection probability P do not influence the stability of the spiral wave and just provide some perturbations.

The first non-equilibrium phase transition critical point ($\rm CP_1$) revealed by Fig. 2(a) occurs at $P = 0.07$, where some $\langle N_{\rm tip}\rangle$s in fifty samples are larger than one and multi-tips of spiral waves can be detected. It indicates that spiral waves in these network structures begin to break, multi-tip spirals form and control the whole system. A typical spatiotemporal pattern of broken spiral waves with multi-tips at $P = 0.07$ is shown in Fig. 1(c). Here we should mention that not all the network structures in 50 samples at $P = 0.07$ can cause the spiral wave to be broken. A perfect spiral wave stays stable in most of samples (48 samples in the simulation) and only 2 samples with special network structure can induce spiral wave fragmentized. Spiral wave breakup induced by long-range links is due to two reasons. One is that the spiral arms invade the refractory regions, so that the propagation is inhibited and the wave fronts break to form extra tips. The other is that some of the wave arms collide with other excitable waves induced by long-range links and cause spirals breakup.

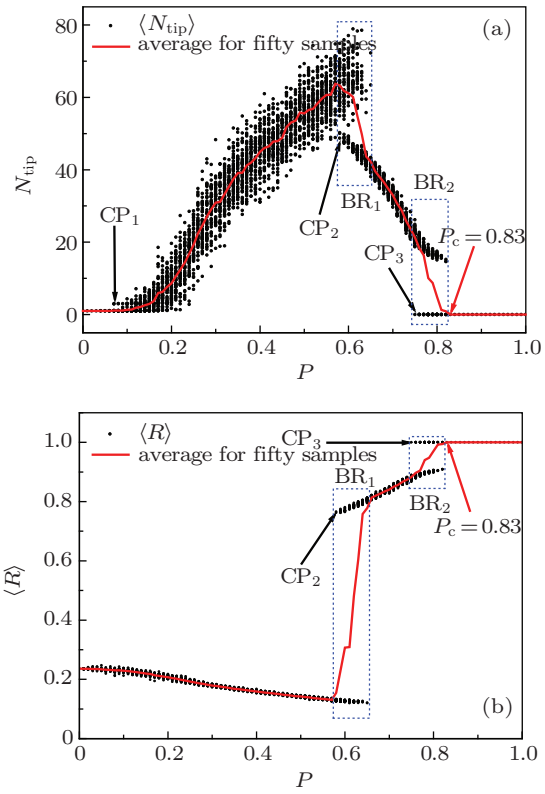


Fig. 2. (colour online) The distributions of the time average of spiral tip number $\langle N_{\rm tip}\rangle$ (a) and the Kuramoto order parameter $\langle R\rangle$ (b) versus the long-range connection probability P are plotted by black dots. Symbol $\langle\ \rangle$ represents time average. The red lines show the average of $\langle N_{\rm tip}\rangle$s (a) and $\langle R\rangle$s (b) for fifty samples. Here $\rm CP_{\it i}$ ($i = 1, 2, 3$) and $\rm BR_{\it j}$ ($j = 1, 2$) mean non-equilibrium phase transition critical points (denoted by black arrowed line) and bistable regions (indicated by blue dashed rectangle), respectively. $P_{\rm c}$ implies the critical connection probability for control.

With the increase of long-range connection probability P, spatiotemporal patterns formed in the excitable small-world network become chaotic. Spiral turbulence patterns with a large number of tips emerge and exist in a wide range of connection probability. One typical spatiotemporal pattern of spiral turbulence at $P = 0.40$ is shown in Fig. 1(d). Note that the spiral turbulence formed in the excitable small-world network is a kind of pseudo turbulence. The differences between pseudo turbulence and real turbulence can be distinguished in two ways. One is the time series of the arbitrary single node in the medium. In the case of pseudo turbulence of Fig. 1(d), the time series of an arbitrary excitable node are nearly periodic as shown in Fig. 3(a). While the chaotic time series displayed in Fig. 3(b) come from the real turbulence with $\varepsilon = 0.08$ in a regular excitable medium without any long-range links. The second difference is the position of the spiral tips. In pseudo turbulence, spiral tips are almost located at the fixed position. But in real turbulence, spiral tips

will move randomly in the 2D space, which is caused by stochastic generation and annihilation of the tips.

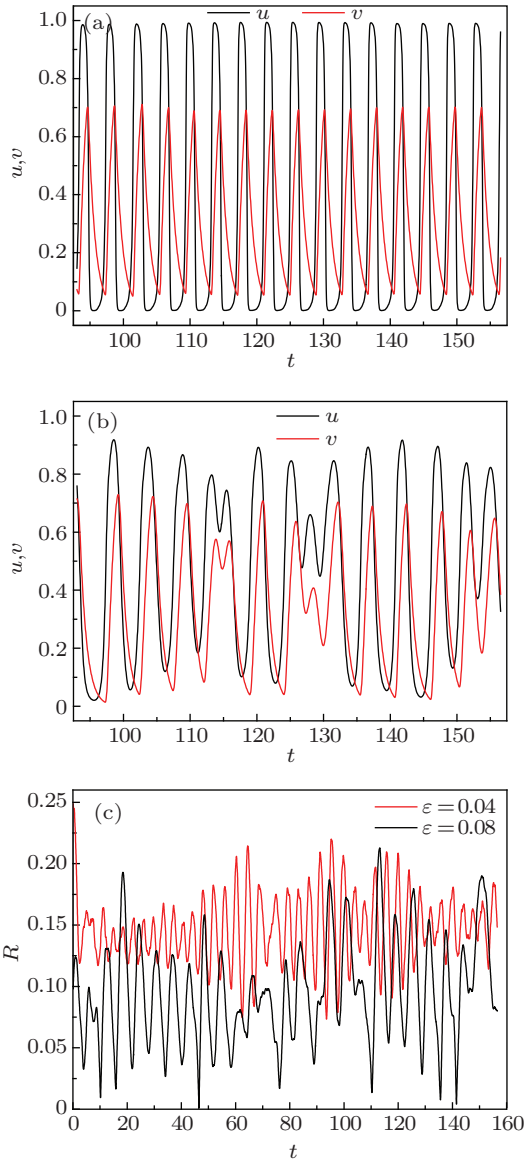


Fig. 3. (colour online) (a) The periodic time series of an arbitrary excitable node of pseudo spiral turbulence of Fig. 1(d) at $P = 0.40$. (b) The chaotic time series of a single node for real turbulence with $\varepsilon = 0.08$ in the regular excitable media without any long-range links. (c) The evolvement of the Kuramoto order parameter $R(t)$ for pseudo spiral turbulence $\varepsilon = 0.04$ of Fig. 3(a) and real turbulence $\varepsilon = 0.08$ of Fig. 3(b).

When long-range connection probability P reaches 0.58, the second non-equilibrium phase transition critical point (CP_2) has been revealed in Fig. 2(a). This critical point can be indicated by the average of $\langle N_{\rm tip}\rangle$s for fifty samples (denoted by red line), which starts to fall from the maximum value at $P = 0.57$. A new kind of spatiotemporal pattern with fewer spiral tips is detected. To further investigate this kind of new pattern, the Kuramoto order parameter $R(t)$ is introduced as[40]

$$R(t) = \frac{1}{N}\left|\sum_{j=1}^{N} \mathrm{e}^{\mathrm{i}\theta_j(t)}\right|, \tag{6}$$

where $N = 10^4$ is the total number of excitable nodes in the whole medium and $\theta_j(t)$ is the phase of the j-th cell at moment t. The Kuramoto order parameter $R(t)$ is used to measure the degree of phase synchronization given by the normalized vector sum of the phases. The value of $R(t)$ close to zero indicates that the phases of the individual excitable cells are evenly distributed and the whole system oscillates asynchronously at them all. While a value of $R(t)$ close to unity indicates all nodes in the 2D space are in phase synchronization, and the whole medium oscillates as a single cell. Figure 2(b) shows the distributions of the time average of the Kuramoto order parameter $\langle R\rangle$ versus the long-range connection probability P by black dots for fifty samples. For a small connection probability, the spiral waves are almost stable and the Kuramoto order parameters are all around 0.23. It indicates that a spiral wave under few long-range links is a kind of asynchronous spatiotemporal pattern. Chaotic pseudo spiral turbulence has formed when long-range connection probability is increased. The whole system exhibits more asynchronous oscillation and $\langle R\rangle$ decreases gradually. The second critical point at $P = 0.58$ can also be indicated by the Kuramoto order parameter in Fig. 2(b), where some of $\langle R\rangle$s in fifty samples jump to a high level and their $\langle N_{\rm tip}\rangle$s are relatively fewer in Fig. 2(a). Thus at this critical point a new kind of highly synchronous oscillation state with fewer spiral tips emerges. One synchronous oscillation state has been displayed in Fig. 1(e) at $P = 0.70$. Lots of nodes in the whole medium oscillate synchronously (shown by white regions), and only a few cells oscillate asynchronously (shown by black regions). The whole system exhibits synchronous oscillation.

From Figs. 2(a) and 2(b), we can find that in the small region of $0.58 \leq P \leq 0.65$ pseudo spiral turbulence and synchronous oscillations coexist at the same long-range connection probability. In fifty samples we can obtain pseudo spiral turbulence for some samples while we get synchronous oscillations for others due to different network structures and this kind of bistable region (BR) is indicated by blue dashed rectangle. So pseudo spiral turbulence and synchronous oscillations coexist in BR_1. As connection probability P increases, $\langle N_{\rm tip}\rangle$ shown in Fig. 2(a) decreases while $\langle R\rangle$ displayed in Fig. 2(b) increases and the whole system oscillates more synchronously. When long-range

connection probability P reaches 0.75, the third non-equilibrium phase transition critical point (CP_3) can be found in Figs. 2(a) and 2(b). Some of the Kuramoto order parameters shown in Fig. 2(b) reach unity and all excitable nodes in the 2D space achieve phase synchronization. The whole system oscillates as a single node. Because of the non-sustained oscillation of the excitable node, the whole medium starts to damp as phase synchronization is achieved. Therefore, the homogeneous rest state emerges and $\langle N_{\rm tip}\rangle$ falls to zero. In simulation we find that the rest state and the synchronous oscillations can coexist in BR_2 for $0.75 \leq P \leq 0.82$. In this bistable region, with the same initial condition and same connection probability P, in some cases, all nodes will excite almost at the same time, and damp quickly to their rest state together at last. Thus there is not any node which could excite again after that to sustain the oscillation of the system (i.e., the homogenous rest state is obtained). While in other cases not all of the nodes can be excited at the same time because the topological structure can be different even in the same connection probability P, and thus the remanent nodes could excite after the synchronous oscillation and sustain the system oscillating forever (i.e., the synchronous oscillation can be achieved). That is to say, the bistability results from the difference in the topological structure. When $P \geq 0.83$, the whole system can evolve into the rest state in fifty samples for arbitrary network structures. It means that for a certain type of excitable medium it is not possible to obtain spiral waves due to the presence of long-range links. Therefore, the critical connection probability $P_{\rm c} = 0.83$ can be used to control spiral waves and spiral waves can be controlled by long-range links if the connection probability $P \geq P_{\rm c}$. A final control result at $P = 0.90$ is shown in Fig. 1(f).

Now we look at insight into the evolvement of the Kuramoto order parameter for different spatiotemporal patterns formed in excitable small-world networks. Figure 4 shows the evolvement of $R(t)$ at different long-range connection probability P. For a small connection probability ($P = 0.05$ of Fig. 1(b), denoted by black line), spiral waves are almost stable and $R(t)$ oscillates around 0.23 periodically. A kind of nearly periodic asynchronous spatiotemporal pattern exists in the small-world network with few long-range links. When pseudo spiral turbulence emerges with more long-range links, $R(t)$ oscillates irregularly at a lower level ($P = 0.40$ of Fig. 1(d), denoted by the red line). The chaos of the spatiotemporal pattern can also be reflected by the irregularity of $R(t)$. When synchronous oscillation emerges, $R(t)$ oscillates at a high level after several transient periods ($P = 0.70$ of Fig. 1(e), denoted by the pink line) and the characteristic of quasi-periodic 2 of synchronous oscillation can be revealed by $R(t)$. As connection probability $P \geq 0.83$, $R(t)$ reaches unity quickly ($P = 0.90$ of Fig. 1(f), denoted by the blue line). The system damps to homogeneous rest state after phase synchronization has been achieved in the whole medium. The Kuramoto order parameter not only can reflect the distinct characteristic of spatiotemporal patterns formed in an excitable small-world network with different connection probabilities, but also can identify pseudo spiral turbulence and real turbulence. Figure 3(c) shows the evolvement of $R(t)$ for pseudo spiral turbulence formed in an excitable small-world network ($\varepsilon = 0.04$ of Fig. 3(a), indicated by the red line) and the real turbulence ($\varepsilon = 0.08$ of Fig. 3(b), indicated by the black line). The Kuramoto order parameter oscillates around 0.15 for pseudo spiral turbulence. While for real turbulence, R oscillates irregularly and the minimal value of R closes to zero. Besides the two aspects mentioned above, we can also identify pseudo spiral turbulence and real turbulence by the Kuramoto order parameter.

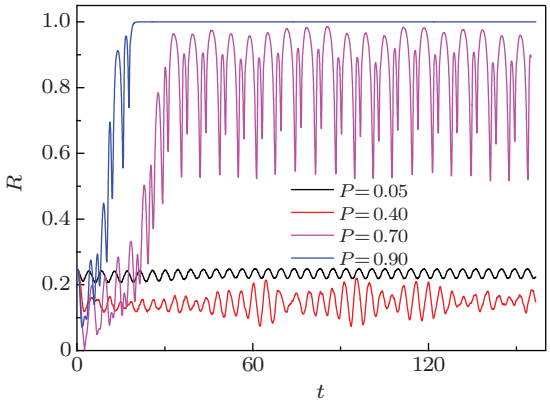


Fig. 4. (colour online) The evolvement of the Kuramoto order parameter $R(t)$ at different long-range connection probability P.

In Fig. 1(f) we can control spiral waves by adding long-range links. Here we would like to kindly point out that there may exist long-range links in cardiac tissue, especially in the atrium, which may trigger atrial fibrillation, e.g., as investigated by Gray and Jalife.[41] Our work provides a different method to suppress spiral waves, which may have practical significance for treatment of arrhythmias. Now we try to control real turbulence by long-range links. A turbulence state shown in Fig. 5(a) is used as our initial condition and parameters are taken the same as above except for $\varepsilon = 0.08$ which is in the real turbulence region.[39] The

distributions of $\langle R\rangle$ versus the long-range connection probability P are plotted in Fig. 5(b) by black dots for fifty samples. By increasing connection probability, $\langle R\rangle$ undergoes non-equilibrium phase transition from low to high. When connection probability P reaches critical probability $P_c = 0.66$, the real turbulence can be controlled into the homogeneous rest state in fifty samples. The evolvement of R at $P = 0.70$ is shown in Fig. 5(c). The Kuramoto order parameter reaches unity quickly after a few transient periods and homogeneous rest state shown in Fig. 5(d) can be obtained after phase synchronization is achieved. In simulation, we find that the critical connection probability P_c is dependent on parameter ε. The relationship between P_c and ε is plotted by black squares in Fig. 6. With the increase of ε, it is easier for the whole medium to achieve phase synchronization and the critical probability decreases.

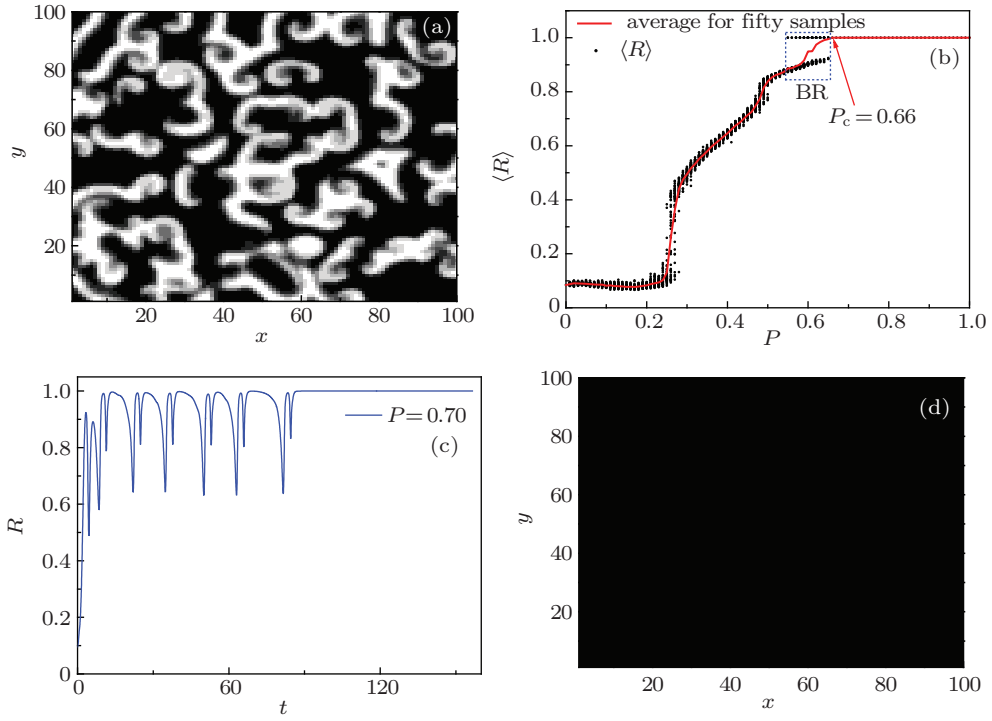


Fig. 5. (colour online) (a) A turbulence state is used as initial condition. (b) The distributions of the time average of the Kuramoto order parameter $\langle R\rangle$ versus the long-range connection probability P are plotted by black dots. The red line shows the average of $\langle R\rangle$s for fifty samples. BR (indicated by the blue dashed rectangle) is the bistable region where synchronous oscillations and homogeneous rest state coexist. And P_c implies the critical connection probability for control. (c) The evolvement of the Kuramoto order parameter $R(t)$ at $P = 0.70$. (d) Homogeneous rest state obtained at $P = 0.70$.

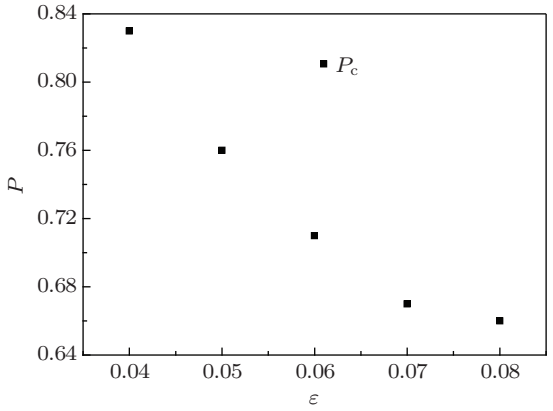


Fig. 6. The relationship between critical connection probability P_c and parameter ε.

3. Conclusion

In conclusion, we have investigated the influence of long-range links on spiral waves in an excitable medium. As the long-range connection probability P increases, spatiotemporal dynamics in an excitable small-world network transform remarkably. Five distinct spatiotemporal patterns, i.e., spiral waves with few perturbations, broken spiral waves, pseudo spiral turbulence, synchronous oscillations, and homogeneous rest state, have been found under different network structures. We use spiral tip number to reveal the non-equilibrium phase transition between different spatiotemporal patterns and the Kuramoto order

parameter is used to identify these patterns and explain the emergence of the rest state. Finally, we can successfully control spiral waves and spiral turbulence by long-range links.

Since spiral wave dynamics in excitable small-world network is a very important topic in wide practical fields, especially in biological systems, a systematic investigation of the influence of long-range links on spiral waves is expected to be useful both for theoretical understandings and practical applications. The distinct spatiotemporal dynamics under different network structures may help us understand complicated oscillation rhythms in biological systems. Moreover, the spiral control method proposed in this paper may have practical significance for treatment of arrhythmias. We do hope that our results may have a useful impact in these fields.

References

[1] Lechleiter J, Girard S, Clapham D and Peralta E 1991 *Nature* **350** 505

[2] Glass L 1996 *Phys. Today* **45** 40

[3] Zaikin A N and Zhabotinsky A M 1970 *Nature* **225** 535

[4] Winfree A T 1972 *Science* **175** 634

[5] Ouyang Q and Flesselles J M 1996 *Nature* **379** 143

[6] Davidenko J M, Pertsov A V, Salomonsz R, Baxter W and Jalife J 1992 *Nature* **355** 349

[7] Kanakov O I, Osipov G V, Chan C K and Kurths J 2007 *Chaos* **17** 015111

[8] Huang X D, Qian Y, Zhang X M and Hu G 2010 *Phys. Rev.* E **81** 051903

[9] Grayalife R A, Pertsov A M and Jalife J 1998 *Nature* **392** 75

[10] Weiss J N, Garfinkel A, Karagueuzian H S, Qu Z L and Chen P S 1999 *Circulation* **99** 2819

[11] Gray R A 2002 *Chaos* **12** 941

[12] Aliev R R and Panfilov A V 1996 *Chaos, Solitons and Fractals* **7** 293

[13] Alonso S, Sagues F and Mikhailov A S 2003 *Science* **299** 1772

[14] Zhang H, Hu B and Hu G 2003 *Phys. Rev.* E **68** 026134

[15] Zhang H, Cao Z J, Wu N J, Ying H P and Hu G 2005 *Phys. Rev. Lett.* **94** 188301

[16] Xiao J H, Hu G, Zhang H and Hu B 2005 *Europhys. Lett.* **69** 29

[17] Qian Y, Song X Y, Shi W, Chen G Z and Xue Y 2006 *Acta Phys. Sin.* **55** 4420 (in Chinese)

[18] Ma J, Ying H P and Li Y L 2007 *Chin. Phys.* **16** 955

[19] Qiu K, Tang J, Ma J and Luo J M 2010 *Chin. Phys.* B **19** 030508

[20] Zhong M and Tang G N 2010 *Acta Phys. Sin.* **59** 1593 (in Chinese)

[21] Gao J Z, Xie L L, Xie W M and Gao J H 2011 *Acta Phys. Sin.* **60** 080503 (in Chinese)

[22] Jeong H, Mason S P, Barabasi A L and Oltvai Z N 2001 *Nature* **441** 41

[23] Camacho J, Guimera R and Amaral L N 2002 *Phys. Rev. Lett.* **88** 228102

[24] Bazhenov M, Timofeev I, Steriade M and Sejnowski T J 1999 *Nature Neuroscience* **2** 168

[25] Steriade M and Timofeev I 2003 *Neuron* **37** 563

[26] Buzsaki G and Draguhn A 2004 *Science* **304** 1926

[27] Mi Y Y, Zhang L S, Huang X D, Qian Y, Hu G and Liao X H 2011 *Europhys. Lett.* **95** 58001

[28] Hemmen J L 2004 *Biol. Cybern.* **91** 347

[29] Huang X Y, Troy W C, Yang Q, Ma H T, Laing C R, Schiff S J and Wu J X 2004 *The Journal of Neuroscience* **24** 9897

[30] Dahlem M A, Schneider F M and Schöll E 2008 *Chaos* **18** 026110

[31] Watts D J and Strogatz S H 1998 *Nature* **393** 440

[32] He D H, Hu G, Zhan M, Ren W and Gao Z 2002 *Phys. Rev.* E **65** 055204R

[33] Qi F, Hou Z H and Xin H W 2003 *Phys. Rev. Lett.* **91** 064102

[34] Roxin A, Riecke H and Solla S A 2004 *Phys. Rev. Lett.* **92** 198101

[35] Yonker S and Wackerbauer R 2006 *Phys. Rev.* E **73** 055206

[36] Sinha S, Saramäki J and Kaski K 2007 *Phys. Rev.* E **76** 015101R

[37] Qian Y, Huang X D, Hu G and Liao X H 2010 *Phys. Rev.* E **81** 036101

[38] Wang C N, Ma J, Tang J and Li Y L 2010 *Commun. Theor. Phys.* **53** 382

[39] Bär M and Eiswirth M 1993 *Phys. Rev.* E **48** 1635R

[40] Steele A J, Tinsley M and Showalter K 2006 *Chaos* **16** 015110

[41] Gray R A and Jalife J 1998 *Chaos* **8** 65